PHYSICAL REVIEW B VOLUME 56, NUMBER 22 1 DECEMBER 1997-II

Magnetic properties of $(m\text{-MPYNN}^+)[\mathrm{Mn_{12}O_{12}(O_2CPh)_{16}(H_2O)_4}]^-$: Enhancement of magnetic relaxation in the $\mathrm{Mn_{12}}$ cluster caused by the organic radical

Keiji Takeda and Kunio Awaga
Department of Basic Science, Graduate School of Arts and Sciences, The University of Tokyo, Komaba, Meguro, Tokyo 153, Japan

(Received 15 July 1997)

We report magnetic properties of the organic/inorganic hybrid salt, $(m\text{-MPYNN}^+)[\mathrm{Mn_{12}O_{12}(O_2CPh)_{16}(H_2O)_4}]^-$ (**2**), where m-MPYNN$^+$ ($=m$-N-methylpyridinium nitronylnitroxide) is a stable organic radical cation with $S=\frac{1}{2}$ and $[\mathrm{Mn_{12}O_{12}(O_2CPh)_{16}(H_2O)_4}]^-$ is a 12-nuclei Mn cluster anion with $S=\frac{19}{2}$, together with the simple salt, $[\mathrm{PPh_4^+}(=$tetraphenylphosphonium$)]$ $[\mathrm{Mn_{12}O_{12}(O_2CPh)_{16}(H_2O)_4}]^-\cdot 2\mathrm{H_2O}$ (**1**). The EPR spectra of **2** are composed of the separate absorption signals of the $\mathrm{Mn_{12}}$ cluster and m-MPYNN$^+$, indicating a negligible exchange interaction between them. Below 65 K, however, an overlap between the absorption tails is clearly observed, suggesting an energy transfer between the resonances. While the temperature dependences of the paramagnetic susceptibilities of **1** and **2** are similar above ~4 K, the two salts show quite different spin dynamics below it. The magnetization curve and ac susceptibility measurements reveal that the organic radical enhances the relaxation of the magnetization of the $\mathrm{Mn_{12}}$ cluster and prevents the magnetization freezing. [S0163-1829(97)06846-X]

I. INTRODUCTION

Nanoscale magnetic materials are now the focus of considerable research.[1–3] The 12-nuclei manganese complexes of the type $[\mathrm{Mn_{12}O_{12}(O_2C}R)_{16}]$ ($R=$methyl, phenyl, etc.), are attracting much interest in the field of molecular magnetism, because of their unusual magnetic properties. A $\mathrm{Mn_{12}}$ cluster molecule was synthesized by Lis in 1980 by means of wet chemistry. He also obtained the crystal structure.[4] In the 1990's various unusual magnetic properties were revealed: the neutral $\mathrm{Mn_{12}}$ clusters possess a high-spin ground state of $S=9-10$ mainly due to a pairwise antiferromagnetic interaction J_1 between neighboring Mn^{3+} ($S=2$) and Mn^{4+} ($S=\frac{3}{2}$) ions in the cluster molecule.[5–7] Except this interaction, the cluster involves another three pairwise exchange interactions, J_2-J_4, that are weaker than J_1, but are believed to bring about almost continuous excited states of different spin multiplicity just above the high-spin ground state.[6] Another character is a uniaxial magnetic anisotropy which is expressed by the zero-field splitting parameter D of $0.6-0.75$ K.[5–7] The combination of the high-spin multiplicity and the magnetic anisotropy gives rise to a potential barrier of DS^2 between the up- and down-spin states.[8] At low temperatures the rotation of the magnetic moments is not free and the friction accompanied by it brings about a hysteresis loop of magnetization curve and appearance of the imaginary component of ac susceptibility.[7,9,10] Very recently magnetization tunneling through the barrier was discovered on the oriented single crystals of $[\mathrm{Mn_{12}O_{12}(O_2CCH_3)_{16}(H_2O)_4}]$.[11–14] While these properties are considered to originate in the single cluster molecule, it is interesting to see how they are affected by the environment around the $\mathrm{Mn_{12}}$ cluster. In addition, since the nanoscale magnetic materials are also attracting interest as a building block of more unusual magnetic materials, it is important to elucidate the intermolecular interactions of the $\mathrm{Mn_{12}}$ clusters.

A stable organic radical family, nitronylnitroxide, has been studied extensively, because of its potential ferromagnetic interactions.[15] The materials are so stable that it is easy to produce ionic nitronylnitroxides by putting a cationic or anionic moiety on the α carbon. The cation, m- or p-N-methylpyridinium nitronylnitroxide (abbreviated as m- or p-MPYNN$^+$, respectively), yields interesting spin systems, such as Kagomé antiferromagnet,[16,17] molecular spin ladder,[18] and so on[19] in combinations with various counter anions. In this work, a hybrid salt of the m-MPYNN$^+$ cation and the $[\mathrm{Mn_{12}O_{12}(O_2CPh)_{16}(H_2O)_4}]^-$ anion was prepared, and its magnetic properties were studied by means of dc and ac magnetic susceptibility measurements and EPR spectroscopy. We also examined the magnetic properties of $(\mathrm{PPh_4^+})[\mathrm{Mn_{12}O_{12}(O_2CPh)_{16}(H_2O)_4}]^-\cdot 2\mathrm{H_2O}$ where the counter part $\mathrm{PPh_4^+}$ was the nonmagnetic tetraphenylphosphonium, for the purpose of comparison.

II. EXPERIMENTALS

The standard material, $(\mathrm{PPh_4^+})[\mathrm{Mn_{12}O_{12}(O_2CPh)_{16}(H_2O)_4}]^-\cdot 2\mathrm{H_2O}$, was prepared according to the literature method.[7] It was identified by the elemental analyses [Calc(found) for $\mathrm{C_{136}H_{112}O_{50}PMn_{12}}$: C, 50.47(50.41); H, 3.49(3.48)] and the IR spectrum [ν=3061(w), 1595(m), 1557(s), 1417(s), 719(s), 677(m), 657(m), 614(m) cm^{-1}]. The hybrid salt of m-MPYNN$^+$ and $[\mathrm{Mn_{12}O_{12}(O_2CPh)_{16}(H_2O)_4}]^-$ was obtained by the same method using m-MPYNN$^+\mathrm{I}^-$ instead of $\mathrm{PPh_4^+I^-}$: To a stirred solution of $[\mathrm{Mn_{12}O_{12}(O_2CPh)_{16}(H_2O)_4}]$ (250 mg) in $\mathrm{CH_2Cl_2}$ (8 ml) was added solid m-MPYNN$^+\cdot\mathrm{I}^-$ (33 mg) under a $\mathrm{N_2}$ inert condition. The solution was stirred for 10 min and then small amounts of brown solid were removed by filtration. On the top of the filtrate surface was slowly added EtOAc/$\mathrm{Et_2O}$ (2:1, 12 ml) and the mixture was stored for one night. 120 mg of black plate crystals of $(m\text{-MPYNN}^+)[\mathrm{Mn_{12}O_{12}(O_2CPh)_{16}(H_2O)_4}]^-$ were collected by filtration. Preliminary x-ray crystal analyses on the crystals gave the lattice parameters, *monoclinic*, $a=18.60$ Å, $b=20.09$ Å, $c=21.96$ Å, $\beta=91.3°$, and $V=8203$ Å^3. However the crystal was unstable probably due to evaporation of crystal solvents and became mosaic rather quickly, so we could not carry out the full structural analyses. The mosaic sample dried in vacuo, seemed to be still hydroscopic, analyzing for $(m\text{-MPYNN}^+)[\mathrm{Mn}_{12}\mathrm{O}_{12}(\mathrm{O}_2\mathrm{CPh})_{16}(\mathrm{H}_2\mathrm{O})_4]^-$ [Calcd(found) for $\mathrm{C}_{125}\mathrm{H}_{107}\mathrm{N}_3\mathrm{O}_{50}\mathrm{Mn}_{12}$: C, 48.27(48.08); H, 3.47(3.64); N, 1.35(1.58)]. The agreement between the observation and calculation indicated that there was no chemical decomposition after the sample has become mosaic. The IR spectrum showed the presence of the Mn_{12} cluster anion [$\nu=3063$(w), 1596(m), 1553(s), 1416(s), 719(s), 676(m), 661(m), 613(m) cm^{-1}], but the bands of m-MPYNN$^+$ were not clear, because of superimposition of the cluster bands that were much stronger than those of m-MPYNN$^+$.

X-band EPR were recorded on a JES-RE2X spectrometer equipped with an Oxford continuous He gas-flow cryostat. The magnetic susceptibility and magnetization measurements were carried out on a Quantum Design MPM5S superconducting quantum interference device susceptometer. The samples for the measurements were pasted with grease in the sample tubes in order to avoid the movement of the sample caused by the strong magnetic force due to the high-spin multiplicity.

III. EPR SPECTROSCOPY

The temperature-variable X-band EPR measurements were performed on the standard sample $(\mathrm{PPh}_4^+)[\mathrm{Mn}_{12}\mathrm{O}_{12}(\mathrm{O}_2\mathrm{CPh})_{16}(\mathrm{H}_2\mathrm{O})_4]^- \cdot 2\mathrm{H}_2\mathrm{O}$ (**1**) and the nitronylnitroxide salt $(m\text{-MPYNN}^+)[\mathrm{Mn}_{12}\mathrm{O}_{12}(\mathrm{O}_2\mathrm{CPh})_{16}(\mathrm{H}_2\mathrm{O})_4]^-$ (**2**) in the temperature range 7–270 K. The spectra of **1** at representative temperatures are shown in Fig. 1(a). An absorption signal appears below ~65 K at $H=600$ Oe ($g=10.5$). As briefly described in the literature,[7] the peak intensity grows with increasing temperature up to 20 K, whereupon it begins to decrease until it disappears at ~65 K. Because of the complicated electronic structure of the Mn_{12} cluster,[6] it is hard to identify the spin states which are relevant to the absorption, but the behavior suggests that it is from a thermally populated excited state. Figure 1(b) shows the spectra of **2**, where the signal intensities at the higher three temperatures are reduced to one-sixth. The absorption manifesting itself at $H=600$ Oe below 65 K is easily assigned to that of the Mn_{12} cluster. The electronic structure of the Mn_{12} cluster in **2** is similar to that in **1** whose the ground state has been reported to be of $S=\frac{19}{2}$.[7] Further the absorption observed at $H=3200$ Oe ($g=2$) in the whole temperature range is ascribed to that of m-MPYNN$^+$. Figures 2(a) and 2(b) show the g factor and the peak-to-peak linewidth ΔH_{pp} for the absorption, respectively, plotted as a function of temperature. At 270 K, $g=2.006$ and $\Delta H_{\mathrm{pp}}=73$ Oe. The g factor is nearly equal to those of the simple m-MPYNN$^+$ salts, while the value of ΔH_{pp} is larger than the usual ones.[16] The line broadening would be caused by the inhomogeneous field around m-MPYNN$^+$ created by the high-spin clusters. The NO groups of nitronylnitroxide often operate as a ligand to various metal ions, such as Mn and Cu ions.[20–22] Since the signals of m-MPYNN$^+$ and the Mn_{12} cluster are observed separately, it can be concluded that there is no chelation of the NO groups to the Mn ions. This indicates that the exchange interaction between m-MPYNN$^+$ and $[\mathrm{Mn}_{12}\mathrm{O}_{12}(\mathrm{O}_2\mathrm{CPh})_{16}(\mathrm{H}_2\mathrm{O})_4]^-$ is not significant. As the temperature is decreased from 270 to 65 K, the g-factor shows a slight increase, followed by a considerable increase below it. The linewidth shows slight narrowing, as the temperature is decreased down to 100 K, below which remarkable broadening takes place. Since an overlap between the absorption tails of the Mn_{12} cluster and m-MPYNN$^+$ is clearly present in the spectra below 65 K, the observed g-factor shift and linewidth broadening at the low tempera-

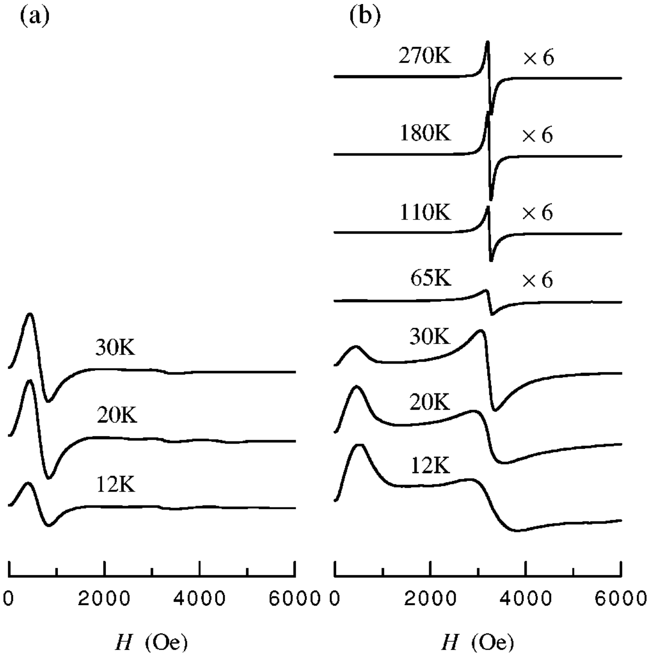

FIG. 1. EPR spectra of the polycrystalline samples of **1** (a) and **2** (b) at representative temperatures. In Fig. 1(b) the signal intensities at the higher three temperatures are reduced one-sixth.

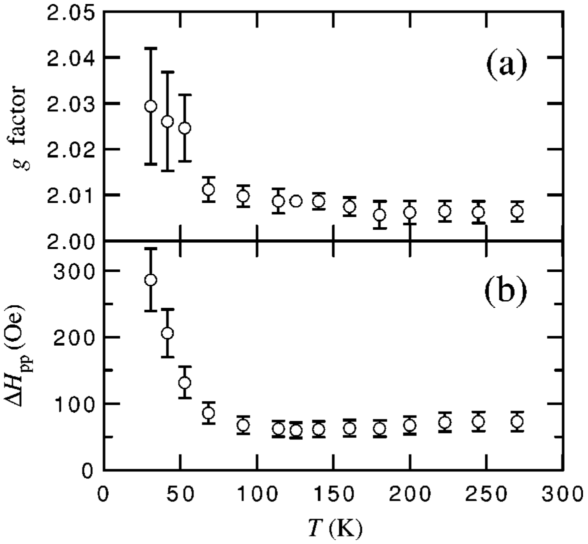

FIG. 2. Temperature dependence of the g factor (a) and the linewidth ΔH_{pp} (b) for the absorption of m-MPYNN$^+$ in **2**.

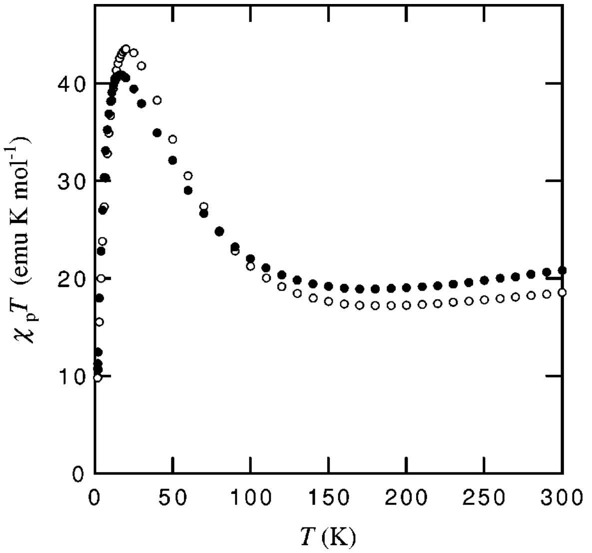

FIG. 3. Temperature dependence of the product χ_pT for the polycrystalline samples of **1** (open circles) and **2** (closed circles) at 1.7 K, where χ_p is the paramagnetic susceptibility.

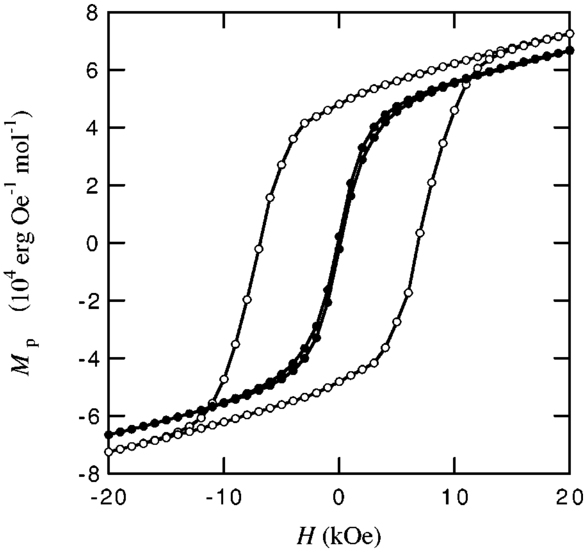

FIG. 4. Magnetization curves for the polycrystalline samples of **1** (open circles) and of **2** (closed circles) at 1.7 K.

tures can be explained in terms of the cross relaxation.[23–25] It is established that organic radicals possess enhanced spin-lattice interactions, because of their ‘‘soft’’ molecular structures: the spin states in them are affected by the molecular vibration or so on, compared with those in inorganic substances. When there is an energy transfer between the two resonances of the inorganic and organic spin species, the probability of an energy flow from spin to lattice is enhanced through the strong spin-lattice interaction on the organic molecule. The cross relaxation in **2** is supported by the fact that the signal of the Mn_{12} cluster in **2** is broader than the corresponding signal of **1**.

IV. dc MAGNETIZATION

The dc magnetic susceptibilities of **1** and **2** were examined in the temperature range 1.7–300 K. The paramagnetic susceptibilities χ_p were obtained by compensating the Pascal’s diamagnetic susceptibility of -1.63×10^{-3} emu mol^{-1} for **1** or of -1.72×10^{-3} emu mol^{-1} for **2**. The open circles in Fig. 3 represent the temperature dependence of the product χ_pT for **1**. The value shows a gradual decrease with decreasing temperature down to 180 K and, after passing through a broad minimum, it increases rather quickly. The behavior is quite similar to those of the other Mn_{12} high-spin molecules[6,7] and is caused by the antiferromagnetic interaction in the Mn_{12} cluster. The closed circles in Fig. 3 show the results on **2**. The value of **2** at 300 K is slightly larger than that of **1**, probably due to the contribution from the organic radical. The temperature dependence of χ_pT for **2** is similar to that for **1**, although the two plots have an intersection at ~80 K. There are several possibilities which can explain the intersection; an intermolecular interaction between m-MPYNN$^+$’s, modification in the intramolecular magnetic parameters of the Mn_{12} cluster, or so on.

The field dependence of the dc magnetizations was examined at 1.7 K in the field up to 20 kOe. The open circles in Fig. 4 show the magnetization curve for **1**. The plots make a large hysteresis loop whose coercive field is about 7000 Oe. The closed circles represent the results on **2**. Surprisingly the loop almost disappears and the coercive field is less than 100 Oe which is smaller than that of **1** by two orders of magnitude. The hysteresis loop or, in the other words, the spin dynamic of the Mn_{12} cluster, is seriously affected by the organic radical, which must neighbor on the clusters in the solid.

V. ac MAGNETIC SUSCEPTIBILITY

The real (χ') and imaginary (χ'') components of the ac magnetic susceptibilities were recorded for the polycrystalline samples of **1** and **2** in the temperature range 1.7–8 K. The data for **1** were taken in zero dc field with a 2 Oe ac field at 10, 30, 99.9, 250, 499, and 997 Hz. In Figs. 5(a) and 5(b) are shown the plots of $\chi'T$ vs T and χ'' vs T for **1**, respectively. The insets show the behavior in the 1.7–3.0 K range in an enlarged scale, where the data at the higher three frequencies are omitted because of their poor S/N ratio. The value of $\chi'T$ decreases below 6 K and that of χ'' makes a maximum simultaneously, showing systematic frequency dependence. The decrease in $\chi'T$ with the appearance of χ'' is associated with the freezing process of the magnetization: as the temperature is decreased, the thermal energy is reduced to a point where the magnetic moment (magnetization) of the Mn_{12} cluster cannot follow the oscillating field. And when the temperature is decreased more, the motion of the magnetic moment is completely frozen and the values of both χ' and χ'' become small. The neutral Mn_{12} clusters are known to exhibit two maximums in χ'',[26] although the reason for them has not been given yet. Actually we found another small maximum in χ'' at ~2 K even for the anion cluster **1** (see the insets in Fig. 5). The anion Mn_{12} clusters have been reported to show only one maximum in χ'' at ~5 K.[7]

In the process of the magnetization freezing in the uniaxial single-domain magnetic particle, the thermal relaxation time τ can be expressed by the following equation:[8,9,27]

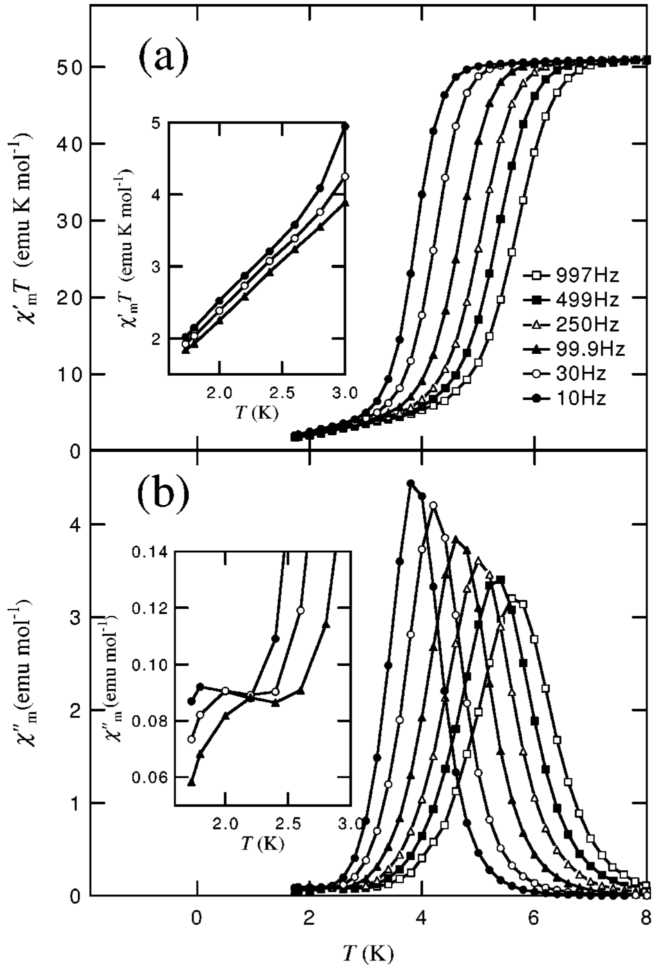

FIG. 5. Temperature dependence of the ac magnetic susceptibility for the polycrystalline sample of **1** at various frequencies; (a) plot of $\chi' T$ vs T, where χ' is the real component, (b) plot of χ'' vs T, where χ'' is the imaginary component. The insets show the dependence in the 1.7−3 K range on an enlarged scale.

$$\tau = \tau_0 \exp\left(\frac{\Delta E}{k_B T}\right), \qquad (1)$$

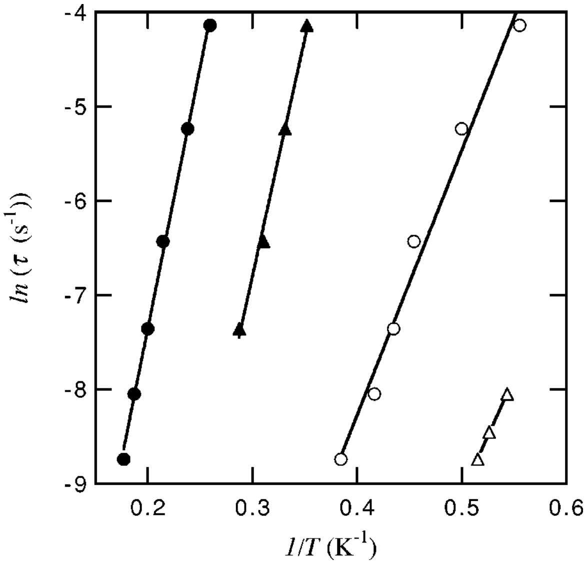

FIG. 6. Arrhenius' plots of the relaxation times τ obtained from the frequency dependence of the ac magnetic susceptibility. The closed and open circles show the results on the HT and LT relaxation processes in **1**, respectively. The closed and open triangles do those on the HT and LT relaxation processes in **2**, respectively. The solid lines are the best fits to the Arrhenius equation.

where τ_0 is the prefactor, k_B is the Boltzmann constant, and ΔE is the potential barrier between the up- and down-spin states. The temperature dependence of τ can be obtained from the frequency dependence of the maximum in χ'', where $\tau = 1/[2\pi\nu_{ac}(=\text{frequency of the ac field})]$ and T is the temperature of maximum in χ''. The open circles and triangles in Fig. 6 show the Arrhenius' plots for the higher- (HT) and lower-temperature (LT) freezing processes in **1**, observed at ~5 and 2 K, respectively. The two plots show a linear relation between lnτ and $1/T$, suggesting that the relaxations are mainly governed by the thermal effect. The effect of the magnetization tunneling discovered recently,[11–14] seems small. The obtained values of τ_0 and ΔE are listed in Table I. ΔE of the LT relaxation is about half as much as that of the HT one. The bulk spin dynamics must be governed by the HT freezing process which makes the main maximum in χ''. The blocking temperature T_B is evaluated to be 2.7 K using the data on the HT maximum, when T_B is defined as the temperature of $\tau = 100$ s. The value is quite consistent with the large hysteresis loop of the magnetization for **1** observed at 1.7 K which is below the estimated T_B.

The ac susceptibilities for **2** were recorded in zero dc field with a 2 Oe ac field at 10, 30, 99.9, 250, 499, 750, and 997 Hz. Figures 7(a) and 7(b) show the temperature dependences of $\chi' T$ and χ'' for **2**, respectively. The insets show the behavior in the 1.7–4.0 K range at the frequencies of 10, 30, and 99.9 Hz in an enlarged scale. There is a relatively constant value of $\chi' T = 41$ emu K mol^{-1} above 4 K without depending on the frequency. When the temperature is decreased from 4 K, $\chi' T$ shows a small decrease in the 2.5–4.0 K range, followed by a drastic decrease with systematic frequency dependence. The values of χ'' make a small and large maximums at 3 and at 2 K or below, respectively, in accord to the decreases in $\chi' T$. It is characteristic that the intensity ratio between the HT and LT maximums in χ'' for **2** is contrary to that for **1**. The closed circles and triangles in Fig. 6 show the Arrhenius' plots for the HT and LT freezing processes in **2**, respectively. The two plots show a linear relation

TABLE I. The potential barrier ΔE, the prefactor τ_0 and the blocking temperature T_B for the HT and LT relaxation processes in **1** and **2**.

	1	**2**
HT relaxation		
$\Delta E/k_B$ (K)	55	50
τ_0 (s)	1.0×10^{-8}	3.0×10^{-10}
T_B (K)	2.7	(1.9)
LT relaxation		
$\Delta E/k_B$ (K)	28	25
τ_0 (s)	3.4×10^{-9}	5.0×10^{-10}
T_B (K)	(1.3)	1.0

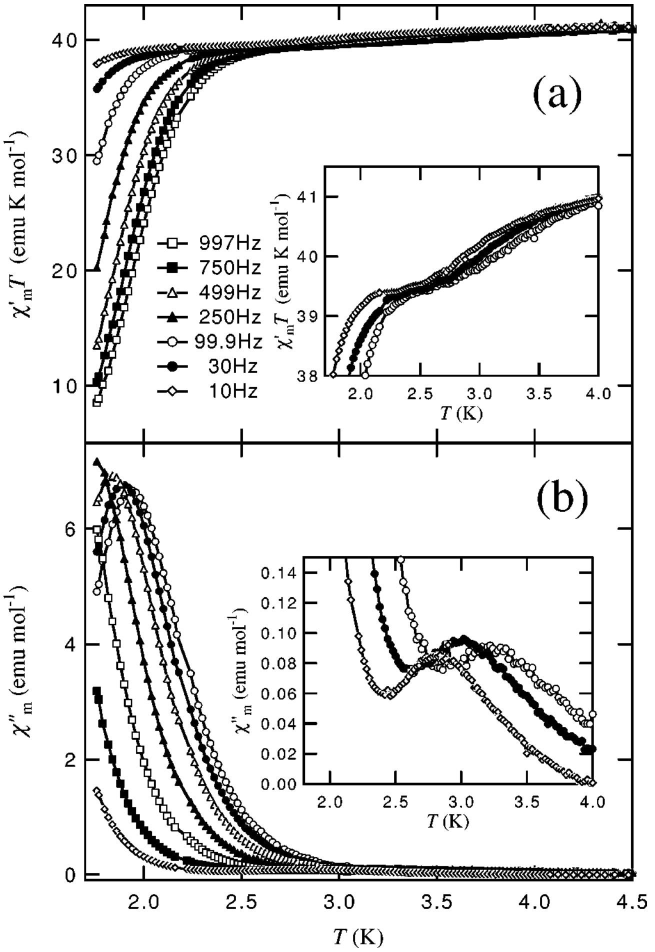

FIG. 7. Temperature dependence of the ac magnetic susceptibility for the polycrystalline sample of **2** at various frequencies; (a) plot of $\chi' T$ vs T, where χ' is the real component, (b) plot of χ'' vs T, where is χ'' is the imaginary component. The insets show the dependence in the 1.7−4 K range on an enlarged scale.

between $\ln\tau$ and $1/T$, from which the values of τ_0 and ΔE are obtained as shown in Table I. The ratio between ΔE for the LT and HT processes is almost 1:2 in **2**, as well as that in **1**, while, in each process, the value of ΔE for **2** is smaller than that for **1** by $\sim 10\%$. The parameter ΔE is caused by the spin multiplicity and the magnetic anisotropy in the Mn_{12} cluster, so that it is natural that ΔE is not very affected by the organic radical. On the other hand, τ_0 for **2** in each process is shorter than that for **1** by one or two orders of magnitude. As for the parameter τ_0 which is related to the microscopic mechanism or pathway of the relaxation, the dominant contribution from the spin-lattice interaction over the spin-spin interaction is theoretically pointed out.[8] As demonstrated in the EPR measurements, the organic radical and the Mn_{12} cluster are practically connected from the viewpoint of the energy transfer. This and the strong spin-lattice interaction on the organic radical would be responsible for the much shorter τ_0 values for **2**.

Since the bulk magnetic properties of **2** are governed by the LT freezing process, T_B is estimated to be 1.0 K for **2**. This is consistent with the small hysteresis loop of the magnetization of **2** found at 1.7 K, which is above T_B. The crucial difference in the magnetization curve at 1.7 K between **1** and **2** can be simply understood by the low-temperature shift of T_B in **2**. However, it is worth noting that the low-temperature shift of T_B is brought about mainly by the suppression of the HT relaxation in **2**. The microscopic origin of the two maximums in χ'' is not clear at this stage and it is hard to discuss how their intensities are determined. However, it is obvious that the organic radical can change the intensity ratio, and it will be a future problem to clarify the origin, taking advantage of the hint dropped by the organic radical.

We described two kinds of the magnetic relaxations in **2**; the relaxation in the EPR and the rotation of the magnetization toward a stable direction. The former occured in the paramagnetic temperature range, after an excess energy was given by an electromagnetic field, while the latter did in the magnetization-freezing temperature range, when an external field was applied. It was interesting that they were commonly enhanced by the organic radical.

VI. SUMMARY

We studied the magnetic properties of $(PPh_4^+)[Mn_{12}O_{12}(O_2CPh)_{16}(H_2O)_4]^- \cdot 2H_2O$ (**1**) and $(m\text{-}MPYNN^+)[Mn_{12}O_{12}(O_2CPh)_{16}(H_2O)_4]^-$ (**2**). The EPR spectra of **2** showed little exchange interaction between the nitronylnitroxide and the Mn_{12} cluster, but suggested the energy transfer between them. Although χ_p of **1** and **2** showed similar temperature dependence above ~ 4 K, they exhibited quite different spin dynamics below it: at 1.7 K, the magnetization curve of **2** exhibited little hysteresis in contrast to the large hysteresis loop of **1**. The temperature and frequency dependences of the ac susceptibilities indicated the characteristic decrease in T_B and the shortening of τ_0 for **2**.

ACKNOWLEDGMENTS

This work was supported by the Grant-in-aid for Scientific Research from the Ministry of Education, Science, and Culture, of the Japanese government and by the CREST (Core Research for Evolutional Science and Technology) of the Japan Science and Technology Corporation (JST).

---

[1] D. Gatteschi, A. Caneschi, L. Pardi, and R. Sessoli, Science **265**, 1054 (1994).

[2] D. D. Awschalom and D. P. DiVincenzo, Phys. Today **48** (4), 43 (1995).

[3] S. Gider, D. D. Awschalom, T. Douglas, S. Mann, and M. Chaparala, Science **268**, 77 (1995).

[4] T. Lis, Acta Crystallogr., Sect. B: Struct. Crystallogr. Cryst. Chem. **36**, 2042 (1980).

[5] A. Caneschi, D. Gatteschi, and R. Sessoli, J. Am. Chem. Soc. **113**, 5873 (1991).

[6] P. D. W. Boyd, Q. Li, J. B. Vincent, K. Folting, H.-R. Chang, W. E. Streib, J. C. Huffman, G. Christou, and D. N. Hendrickson, J.

Chem. Soc. **110**, 8537 (1988); R. Sessoli, H.-L. Tsai, A. R. Schake, S. Wang, J. B. Vincent, K. Folting, D. Gatteschi, G. Christou, and D. N. Hendrickson, *ibid.* **115**, 1804 (1993).

[7] H. J. Eppley, H.-L. Tsai, N. de Vries, K. Folting, G. Christou, and D. N. Hendrickson, J. Am. Chem. Soc. **117**, 301 (1995).

[8] J. Villain, F. Hartman-Boutron, R. Sessoli, and A. Rettori, Europhys. Lett. **27**, 159 (1994).

[9] R. Sessoli, D. Gatteschi, A. Caneschi, and M. A. Novak, Nature (London) **365**, 141 (1993).

[10] C. Paulsen, J.-G. Park, B. Barbara, R. Sessoli, and A. Caneschi, J. Magn. Magn. Mater. **140-144**, 1891 (1995).

[11] J. R. Friedman, M. P. Sarachik, J. Tejada, and R. Ziolo, Phys. Rev. Lett. **76**, 3830 (1996).

[12] L. Thomas, F. Lionti, R. Ballou, D. Gatteschi, R. Sessoli, and B. Barbara, Nature (London) **383**, 145 (1996).

[13] J. M. Hernandez, X. X. Zhang, F. Luis, J. Tejada, J. R. Friedman, M. P. Sarachik, and R. Ziolo, Phys. Rev. B **55**, 5858 (1997).

[14] F. Luis, J. Bartolome, J. F. Fernandez, J. Tejada, J. M. Hernandez, X. X. Zhang, and R. Ziolo, Phys. Rev. B **55**, 11 448 (1997).

[15] J. Cirujeda, L. E. Ochando, J. M. Amigó, C. Rovira, J. Ruis, and J. Veciana, Angew. Chem. Int. Ed. Engl. **34**, 55 (1995); T. Akita, Y. Masaki, K. Kobayashi, N. Koga, and H. Iwamura, J. Org. Chem. **60**, 2092 (1995); M. M. Matsushita, A. Izuoka, T. Sugawara, T. Kobayashi, N. Wada, N. Takeda, and M. Ishikawa, J. Am. Chem. Soc. **119**, 4369 (1997), and references therein.

[16] K. Awaga, T. Okuno, A. Yamaguchi, M. Hasegawa, T. Inabe, Y. Maruyama, and N. Wada, Phys. Rev. B **49**, 3975 (1994); M. Hasegawa, A. Yamaguchi, T. Okuno, and K. Awaga, Synth. Met **71**, 1797 (1995); N. Wada, T. Kobayashi, H. Yano, T. Okuno, A. Yamaguchi, and K. Awaga, J. Phys. Soc. Jpn. **66**, 961 (1997).

[17] C. Michaut, L. Ouahab, P. Bergerat, O. Kahn, and A. Bousseksou, J. Am. Chem. Soc. **118**, 3610 (1996).

[18] H. Imai, T. Inabe, T. Otsuka, T. Okuno, and K. Awaga, Phys. Rev. B **54**, 6838 (1996).

[19] H. O. Stumpf, L. Ouahab, Y. Pei, D. Grandjean, and O. Kahn, Science **261**, 447 (1993).

[20] A. Bencini and D. Gatteschi, in *Electron Paramagnetic Resonance of Exchange Coupled Systems* (Springer-Verlag, Berlin, 1990), p. 193.

[21] A. Caneschi, D. Gatteschi, and R. Sessoli, in *Magnetic Molecular Materials*, edited by D. Gatteschi *et al.* (Kluwer, Dordrecht, 1991), p. 215; C. Benelli, A. Caneschi, D. Gatteschi, and L. Pardi, in *Magnetic Molecular Materials*, edited by D. Gatteschi *et al.* (Kluwer, Dordrecht, 1991), p. 233.

[22] A. Caneschi, D. Gatteschi, and P. Rey, Prog. Inorg. Chem. **39**, 331 (1990).

[23] J. A. Hodges, Physica B & C **86-88B**, 1143 (1977).

[24] C. A. Bates, M. Rezki, A. Vasson, A.-M. Vasson, and A. Gavaix, J. Phys. C **14**, 2823 (1981).

[25] R. Furrer and C. A. Hutchison, Jr., Phys. Rev. B **27**, 5270 (1983).

[26] Reference 7 described the presence of two maximums in χ'' at ~ 3 and 6 K for neutral Mn_{12} cluster. Very recently the third one at ~ 2 K was reported in Ref. 14.

[27] S. M. J. Aubin, M. W. Wemple, D. M. Adams, H.-L. Tsai, G. Christou, and D. N. Hendrickson, J. Am. Chem. Soc. **118**, 7746 (1996).